

Video Article

Evaluation of Zika Virus-specific T-cell Responses in Immunoprivileged Organs of Infected *Ifnar1^{-/-}* Mice

Yongli Zhang^{*1,2}, Hangjie Zhang^{*2}, Wenqiang Ma^{*3}, Kefang Liu^{1,2}, Min Zhao⁴, Yingze Zhao², Xuancheng Lu⁵, Fuping Zhang⁶, Xiangdong Li³, George F. Gao^{1,2,4,6}, William J. Liu^{1,2}

¹School of Laboratory Medicine and Life Sciences, Wenzhou Medical University

²NHC Key Laboratory of Medical Virology and Viral Diseases, National Institute for Viral Disease Control and Prevention, Chinese Center for Disease Control and Prevention

³State Key Laboratory of Agrobiotechnology, College of Biological Sciences, China Agricultural University

⁴Research Network of Immunity and Health (RNiH), Beijing Institutes of Life Science, Chinese Academy of Sciences

⁵Laboratory Animal Center, Chinese Center for Disease Control and Prevention

⁶CAS Key Laboratory of Pathogenic Microbiology and Immunology, Institute of Microbiology, Chinese Academy of Sciences

*These authors contributed equally

Correspondence to: Xiangdong Li at xiangdongli@cau.edu.cn, George F. Gao at gaof@im.ac.cn, William J. Liu at liujun@ivdc.chinacdc.cn

URL: <https://www.jove.com/video/58110>

DOI: [doi:10.3791/58110](https://doi.org/10.3791/58110)

Keywords: Immunology and Infection, Issue 140, Zika virus, antigen-specific T cell, vaccination, immunoprivileged organs, tetramer

Date Published: 10/17/2018

Citation: Zhang, Y., Zhang, H., Ma, W., Liu, K., Zhao, M., Zhao, Y., Lu, X., Zhang, F., Li, X., Gao, G.F., Liu, W.J. Evaluation of Zika Virus-specific T-cell Responses in Immunoprivileged Organs of Infected *Ifnar1^{-/-}* Mice. *J. Vis. Exp.* (140), e58110, doi:10.3791/58110 (2018).

Abstract

The Zika virus (ZIKV) can induce inflammation in immunoprivileged organs (e.g., the brain and testes), leading to the Guillain-Barré syndrome and damaging the testes. During an infection with the ZIKV, immune cells have been shown to infiltrate into the tissues. However, the cellular mechanisms that define the protection and/or immunopathogenesis of these immune cells during a ZIKV infection are still largely unknown. Herein, we describe methods to evaluate the virus-specific T-cell functionality in these immunoprivileged organs of ZIKV-infected mice. These methods include a) a ZIKV infection and vaccine inoculation in *Ifnar1^{-/-}* mice; b) histopathology, immunofluorescence, and immunohistochemistry assays to detect the virus infection and inflammation in the brain, testes, and spleen; c) the preparation of a tetramer of ZIKV-derived T-cell epitopes; d) the detection of ZIKV-specific T cells in the monocytes isolated from the brain, testes, and spleen. Using these approaches, it is possible to detect the antigen-specific T cells that have infiltrated into the immunoprivileged organs and to evaluate the functions of these T cells during the infection: potential immune protection *via* virus clearance and/or immunopathogenesis to exacerbate the inflammation. These findings may also help to clarify the contribution of T cells induced by the immunization against ZIKV.

Video Link

The video component of this article can be found at <https://www.jove.com/video/58110/>

Introduction

The ZIKV is a mosquito-borne flavivirus that was first isolated in 1947 in Uganda from a febrile rhesus macaque. Recently, the ZIKV has become a public health emergency, due to its rapid dissemination in the Americas and its unexpected link to microcephaly and Guillain-Barré syndrome^{1,2,3}. From epidemiological data, the ZIKV has been suspected to be the cause of the Guillain-Barré syndrome in around 1 per 4,000 infected adults⁴. Moreover, a correlation between the ZIKV and testes infection/damage in the mouse model has been demonstrated, suggesting that the ZIKV infection, under certain circumstances, can bypass the blood-testis barrier and eventually lead to male infertility⁵. These findings highlight the importance of completely understanding the induction of protective or pathologic immune responses during a ZIKV infection.

Much remains to be learned about the cellular immune responses to the ZIKV. CD4⁺ and CD8⁺ T-cell responses to the capsid, envelope, and nonstructural protein 1 (NS1) have been observed in ZIKV-infected monkeys and humans^{6,7,8}. In mice, several studies have indicated that CD8⁺ T cells play a protective role in controlling the ZIKV replication^{9,10,11}. Importantly, Jurado *et al.* demonstrated that a ZIKV infection results in the breakdown of the blood-brain barrier and perivascular infiltration of CD8⁺ effector T cells within the testes of *Ifnar1^{-/-}* mice. Furthermore, they showed that CD8⁺ T cells instigate ZIKV-associated paralysis and appear to play a role in the neonatal brain immunopathology. In a previous study, we prepared the ZIKV-E₂₉₄₋₃₀₂ tetramer and showed that ZIKV-specific CD8⁺ T cells exist in the brains and spinal cords of ZIKV-infected *Ifnar1^{-/-}* mice, which may have important implications for the design and development of ZIKV vaccines¹⁰.

In response to the urgent need for vaccination to prevent ZIKV infection, several vaccines are in the preclinical stages of development, including RNA vaccines, recombinant vector-based vaccines, and purified protein subunit vaccines. The plasmid DNA vaccine is in phase 1 clinical trials¹². The evaluation of safety and efficacy of ZIKV vaccines is, therefore, important. One advantage of the vaccines is their ability to elicit specific T-cell responses, which may be important for protection against the ZIKV. By using ZIKV-derived T-cell epitope-related tetramers, the T-cell

immunoreactivity induced by an adenovirus-vector-based ZIKV vaccine could be detected in immunized mice, and both M and E glycoproteins were shown to induce robust antigen-specific CD8⁺ T-cell immunoreactivity¹³.

During a virus infection, the recognition of peptide antigens presented by major histocompatibility complex (MHC) molecules to the T-cell receptor (TCR) is an important T-cell-mediated mechanism for protecting the host¹⁴. Based on this theory, tetramer technology is a unique tool to elucidate the roles that antigen-specific T cells play in regulating the immune responses¹⁵. This protocol describes the establishment of the *lfnar1*^{-/-} mouse model for ZIKV infections, and the detection of reactive T cells in the spleen, brain, and testes of the mice by using tetramer technology. Additionally, we used the ZIKV-E₂₉₄₋₃₀₂ tetramer to detect and evaluate T-cell immunoreactivity induced by a ZIKV vaccine (AdC7-M/E) in immunized mice. This study provides guidance for investigating T-cell responses in immunoprivileged organs and provides a reference for the potential applications in the placenta or fetal brain.

Protocol

Animal experiments were approved by the Institutional Animal Care and Use Committee of National Institute for Viral Disease Control and Prevention, China CDC. All experiments were performed following the Institutional Animal Care and Use Committee-approved animal protocols.

1. Virus Infection

1. Keep adult (6 to 8 week-old) *lfnar1*^{-/-} (50% male and 50% female) mice in standard special pathogen-free (SPF) conditions, and allow them regular access to food and water.
2. Infect the *lfnar1*^{-/-} mice with the ZIKV *via* a retro-orbital inoculation of 100 μ L of ZIKV in a phosphate-buffered saline (PBS) buffer containing 1×10^4 focus-forming units (FFUs) of the virus. Similarly, provide control mice with an equal volume of PBS.
CAUTION: Infect the mice under ABSL2 conditions and perform these procedures with virus-infected mice in the biosafety cabinet.
3. Monitor the weight and clinical signs (tremors, staggered march, bilateral flaccid hind limb) of the mice daily for 15 days.

2. Immunization with the ZIKV Vaccine

1. Use *lfnar1*^{-/-} (50% male and 50% female) mice between 6 and 8 weeks of age. Keep the mice in standard SPF conditions of 18–29 °C and a 12 h light/dark cycle with access to food and water.
2. Immunize the *lfnar1*^{-/-} mice with the ZIKV vaccine: inject 100 μ L of AdC7-M/E [4×10^{10} (virus particles)] in PBS buffer *via* an intramuscular injection (the i.m. route) using a 1 mL syringe with a 23-G needle.
3. Similarly, inject control mice with an equal volume of PBS.

3. Isolation of the Monocytes from the Spleen

NOTE: The isolation of the monocytes from the spleen is described as mentioned previously¹⁶.

1. Anesthetize the immunized and ZIKV-infected mice 7 d post-inoculation, using a 5% isoflurane concentration in 100% oxygen (with a flow rate of 1 L/min). Euthanize the mice by cervical dislocation. Then, immediately dip the entire mouse into 75% ethanol.
CAUTION: From this step onward, all experimental procedures should be performed aseptically in a biosafety cabinet.
2. Using needles, fix the limbs of the (euthanized, previously infected/immunized) mice on the foam plate with the abdomen facing up.
3. Cut the skin along the abdominal midline to the thorax with a sterile scalpel, cut the abdominal muscles with scissors, expose the abdominal cavity, and gently remove the liver.
NOTE: The long, dark-red organ to the left of the stomach is the spleen.
4. Remove the spleen, rinse it 3x in PBS to remove any blood, and place it in 1.5 mL of ice-cold Roswell Park Memorial Institute medium (RPMI). Keep the spleen on ice.
5. To generate a single-cell suspension from the spleen, place the organ(s) on a sterile 40 μ m-mesh cell strainer on top of a 50 mL tube and add 2 mL of ice-cold RPMI medium containing 10% fetal bovine serum (FBS). Using the plunger of a 5 mL syringe, mechanically mash the organ(s) and add medium until the organ has been fully ground through the mesh.
6. Transfer the cell suspension to a 15 mL tube and centrifuge it at 600 \times g for 5 min at 4 °C. Remove the supernatant.
7. Resuspend the cells with 5 mL of a red blood cell (RBC) lysis buffer (NH₄Cl, Na₂EDTA, and KHCO₃; see the **Table of Materials**) and incubate the lysis reaction at room temperature for 5–6 min.
8. Stop the RBC lysis with 10 mL of ice-cold RPMI/FBS medium and centrifuge the tube at 600 \times g for 5 min at 4 °C. Remove the supernatant.
9. Resuspend the cells with 10 mL of complete RPMI medium (RPMI with 10% vol/vol FBS and 100 U/mL penicillin-streptomycin). Transfer 10 μ L of the cell suspension to a small tube, mix it with 10 μ L of 0.4% wt/vol trypan blue, and count the number of cells using a hemocytometer.

4. Isolation of Monocytes from the Brain and Testes

1. Anesthetize the ZIKV-infected male mice 7 d post-inoculation, using 5% isoflurane in 100% oxygen (with a flow rate of 1 L/min). Euthanize the mice by cervical dislocation. Then, immediately dip the entire mouse into 75% ethanol.
CAUTION: From this step onwards, all experimental procedures must be performed aseptically in a biosafety cabinet. The isolation of monocytes from the brain and testes is described as mentioned previously¹⁷.
2. Immobilize a (euthanized, previously infected) male mouse in the prone position on a cutting board.
3. Secure the scalp with a straight 1 \times 2 teeth forceps, and use Iris scissors to make a midline incision on the scalp to expose the skull.
4. Clamp the two sides of the orbits with sharp tweezers and fix the brain. Place one tip of sharp Iris scissors into the *foramen magnum* and cut laterally into the skull. Repeat this step for the other side.

5. Use sharp Iris scissors to carefully cut from the same cavity, up the midline, toward the nose. Try to keep the end of the scissors as superficial as possible to avoid injuring the brain.
6. Lift the brain with forceps and use sharp Iris scissors to carefully dissect the cranial nerve fibers. Remove the brain with forceps and place it in a 15 mL tube containing 5 mL of ice-cold RPMI/10% FBS medium.
7. Grab the abdominal skin with forceps and use sharp Iris scissors to make a longitudinal incision through the integument and abdominal wall and expose the lowermost part of the abdomen. Push the testes up to the incision. Gently pull the fat layer with tweezers and expose a globular testis on both sides.
8. Use sharp Iris scissors to carefully dissect the fat layer and epididymis. Place the testes in a 15 mL tube containing 5 mL of ice-cold RPMI/10% FBS medium with forceps.
9. To generate a single-cell suspension from the brain or testes, place the organ on a sterile cell strainer with a 100 μm mesh on top of a 50 mL tube and add 2 mL of ice-cold RPMI/10% FBS medium. Using the plunger of a 5 mL syringe, mash the organ and add medium until the organ has been fully ground through the mesh.
10. Transfer the cell suspension to a 15 mL tube and centrifuge it at 600 x g for 5 min at 4 °C. Remove the supernatant.
11. Resuspend the cells with 5 mL of 30% density gradient medium and, then, add them very slowly to 2 mL of 70% density gradient medium in a 15 mL tube.
12. Switch off the brake and centrifuge the tubes at 4 °C at 800 x g for 30 min. Obtain the lymphocytes from the middle layer.
13. Transfer the interphase to a fresh 15-mL tube, add 10 mL of cold RPMI/10% FBS medium, and centrifuge the tube at 300 x g for 10 min at 4 °C. Remove the supernatant.
14. Resuspend the cells with 10 mL of ice-cold RPMI/FBS medium and centrifuge them at 600 x g for 5 min at 4 °C. Remove the supernatant.
15. Resuspend the cells with 10 mL of complete RPMI medium and count the number of cells as in step 3.9.

5. Tetramer Preparation

1. Construct plasmids expressing the extracellular domains of H-2D^b with a biotinylated site tag on the C-terminus of the $\alpha 3$ domain and the $\beta 2\text{m}$ by using the pET28a vector with an NdeI and XhoI restriction site¹⁸.
2. Express and prepare inclusion bodies of H-2D^b and $\beta 2\text{m}$ as described previously²⁰.
3. **Renature and purify the MHC/peptide complex H-2D^b-E₂₉₄₋₃₀₂**
 1. Prepare 200 mL of a refolding solution [100 mM Tris-HCl (pH 8.0), 400 mM L-arginine, 2 mM EDTA-Na, 5 mM GSG, and 0.5 mM GSSG]. Add protease inhibitors: 2 mL of phenylmethylsulfonyl fluoride (PMSF, stock 100 mM), 100 μL of pepstatin (stock 2 mg/mL), and 100 μL of leupeptin (stock 2 mg/mL). Cool the buffer at 4 °C for 30 min.
 2. Add H-2D^b, $\beta 2\text{m}$, and peptide to the refolding solution.
 1. Inject 500 μL of $\beta 2\text{m}$ dissolved in a guanidine solution (30 mg/mL stock) using a syringe. For this, use a 23 G needle with a 5 mL syringe and inject the $\beta 2\text{m}$ into the refolding solution drop by drop. Keep the solution constantly and slowly stirring at 150 rpm at 4 °C.
 2. After $\beta 2\text{m}$ has been dissolved in the refolding solution, resolve 2 mg of E₂₉₄₋₃₀₂ peptide in 200 μL of DMSO and quickly inject it into the refolding solution using a pipette. Slowly stir the solution at 150 rpm at 4 °C for 15 min.
 3. Inject 1.5 mL of H-2D^b dissolved in a guanidine solution. Keep the stir bar rotating at 150 rpm for the refolding of the H-2D^b at 4 °C for 8–10 h.
NOTE: The solution was placed in a closed box in a cold room.
3. Concentrate the refolded protein in a pressurized chamber with a 10 kDa membrane. Exchange the buffer [20 mM Tris-HCl (pH8.0), 50 mM NaCl] to the chamber and concentrate it to a final volume of 30–50 mL.
4. Transfer the refolding solution to a centrifuge tube and spin it at 2,500 x g for 15 min at 4 °C.
5. Carefully transfer the supernatant to a 10 kDa centrifugal filter and further concentrate it to a final volume of 500 μL at 2,500 x g for 30 min.
6. Transfer the supernatant to a fresh tube and spin it at 12,000 x g for 15 min. Purify the protein with S200 10/300 GL gel filtration chromatography.
7. Collect the MHC complex peak and concentrate it to a final volume of 350 μL .
4. To generate a 500- μL reaction volume for biotinylation, add the reagents in the following order: 100 μL of solution A [0.5M bicine (pH 8.3)], 100 μL of solution B (100 mM ATP, 100 mM MgOAc, 200 μM biotin), 100 μL of extra d-biotin (500 μM biotin), 20 μL of BirA enzyme (60 μg), 0.5 μL of pepstatin (2 mg/mL), and 0.5 μL of leupeptin (2 mg/mL). Incubate the reaction tube overnight at 4 °C.
CAUTION: Do not add any EDTA to the biotinylating reaction.
5. Purify the MHC using a S200 10/300 GL gel filtration column to remove any extra biotin.
6. **Determine the biotinylating efficiency with a streptavidin-shift assay¹⁸**
 1. Prepare three samples, A, B, and C, on ice for 30 min. Then, analyze the results by a 10% SDS-PAGE. Sample A consists of 8 μL of biotinylated MHC molecules and 2 μL of exchange buffer, sample B of 8 μL of biotinylated MHC molecules and 2 μL of streptavidin (20 mg/mL), and sample C of 2 μL of streptavidin (20 mg/mL) and 8 μL exchange buffer.
CAUTION: Do not boil the sample.
7. **Form multimers of the biotinylated MHC molecules.**
 1. Produce tetramer by mixing the biotinylated E₂₉₄₋₃₀₂ peptide-H₂D^b complex with phycoerythrin-labeled streptavidin at a mole ratio of 1:5 to ensure a complete binding of all the biotinylated MHC molecules.
 2. Calculate the amount of streptavidin-conjugate needed for tetramerization.
 1. Determine the moles of the MHC/peptide complexes accounting for the protein concentration and the molar weight (example: 1.8 mg of total protein = 40 nmol).
 2. Calculate the moles of the streptavidin-conjugate needed by dividing the moles of the MHC/peptide by 5 (example: 40/5 = 8 nmol of streptavidin-conjugate).

3. Calculate the amount of streptavidin needed (in μg) depending on the streptavidin-conjugate (example: streptavidin-PE [300,000 g/M] \rightarrow 8 nmol needed = 2,400 g).
3. Divide streptavidin-phycoerythrin into 10 samples. Add each sample to a tube containing the biotinylated $E_{294-302}$ peptide- H_2D^b complex, at an interval of 20 min. After loading the last sample, incubate the reaction tube at 4 °C overnight in dark.
8. Apply the multimerized reagents into a 100 kDa spin tube and concentrate it by centrifugation at 2,000 x g at 4 °C to a volume of <100 μL .
9. Dilute the sample in the spin tube to 4 mL using PBS (pH 8.0) and concentrate it again to <100 μL .
10. Repeat the buffer exchange step in PBS (pH 8.0) 4x.
11. Fill up the total volume again to 500 μL using PBS (pH 8.0). Concentrate the sample to an estimated concentration of 2–2.5 mg/mL at 2,000 x g at 4 °C. Store the sample in the dark at 4 °C.

6. Flow Cytometry

1. Incubate the cell suspensions (from step 3.9 and/or step 4.15) at 4 °C with 0.1 μL of anti-murine CD16/CD32 Fc-Receptor blocking reagent per 20 μL (dilution factor 1:200) for 10 min, to prevent any unspecific binding.
2. Centrifuge the tetramer tube at 20,000 x g for at least 15 min at 4 °C.
3. Add 20 μL of the cell suspension to a 96-well plate containing 1 x 10⁶ cells each well.
4. Prepare a sufficient volume of the $E_{294-302}$ tetramer mix to stain all experimental tubes. Prepare an excess of 15% of the total volume of this mix to account for pipetting errors. Dilute the $E_{294-302}$ tetramers (2 mg/mL, 1 $\mu\text{L}/\text{test}$) in FACS buffer (PBS, 0.5% FBS) so that 20 μL of the $E_{294-302}$ tetramer mix is added to each test.
5. Add 20 μL of the $E_{294-302}$ tetramer mix to the 96-well plate. By the end of this step, the final volume in each well should be 40 μL . Incubate the plate in the dark at room temp for 30 min.
6. Add primary antibodies (FITC-conjugated or APC-conjugated anti-CD3 (0.2 mg/mL), PerCP-conjugated anti-CD8 (0.2 mg/mL)) at 1 $\mu\text{L}/\text{test}$ to the cell suspension and, then, incubate it at 4 °C for 30 min in the dark.
7. Wash the cells 2x with 2 mL of FACS buffer and centrifuge them at 600 x g for 5 min. Carefully aspirate the supernatant and resuspend the cells with 200 μL of FACS buffer.
8. Store the samples temporarily at 4 °C in the dark until the flow cytometric analysis.
9. **Use the following gating strategy for the flow cytometric analysis.**
 1. Create a gate on diagonally clustered singlets by plotting a forward scatter (FSC) versus side scatter (SSC) area.
 2. Then, gate on CD3⁺ cells by side scatter (SSC) versus CD3; next, gate on CD3⁺ CD8⁺ cells; finally, outline CD8⁺ tetramer⁺ cells¹⁹.

7. Histopathology, Immunofluorescence, and Immunohistochemistry Assay

1. **Histopathology assay**
 1. Collect the brain and testis tissues of the ZIKV-infected *Irfar1*^{-/-} mice 7 d post-inoculation and fix them in 4% neutral-buffered formaldehyde.
CAUTION: Paraformaldehyde is toxic; wear appropriate personal protective equipment.
 2. Embed the tissue in paraffin.
 3. Section the tissue at 5 μm using a vibratome.
 4. Stain the tissue with hematoxylin and eosin (H&E).
2. **Immunohistochemistry assay**
 1. Deparaffinize, rehydrate, and antigen-retrieve the tissue sections, based on procedures described previously²¹.
 2. Treat the tissue sections with 3% H_2O_2 in PBS (pH 7.6) for 10 min and block them with 1% bovine serum albumin (BSA) for 10 min.
 3. Incubate the tissue sections with rat anti-mouse CD3 antibody (dilution: 1/1,000) for 8 h at room temperature and, then, incubate them at 4 °C overnight.
 4. Rinse the tissues with PBS and, then, incubate them with 3 drops of biotinylated secondary antibody (dilution: 1/1,000) for 2 h at room temperature, followed by 3 drops of avidin-biotin-peroxidase (dilution: 1/200) at room temperature for 30 min.
 5. Bind, with 3 drops of 3, 3'-diaminobenzidine tetrahydrochloride (dilution: 1/1,000), as described previously²².
 6. Counterstain the tissue sections with Mayer's hematoxylin.
3. **Immunofluorescence assay**
 1. Air-dry the frozen testis sections (6 μm) for 10 min at room temperature.
 2. Fix them with ice-cold acetone for 10 min.
 3. Wash the sections with PBS for 3x and block them with a blocking buffer (1% BSA, 0.3% Triton, 1x PBS) at 37 °C for 30 min.
 4. Incubate the tissue sections with primary antibody (Z6) (20 $\mu\text{g}/\text{mL}$) at 4 °C overnight.
 5. Rinse the tissues with PBS and apply the secondary antibody (dilution factor: 1/200) for 1 h at 37 °C.
 6. Wash the tissue sections with PBS and counterstain them for nuclei using 4', 6-diamidino-2-phenylindole (DAPI) (dilution factor: 1/1,000), following the manufacturer's instructions.

Representative Results

Following these methods, we have developed a murine model for ZIKV infections. *lfnar1*^{-/-} mice at 6–8 weeks of age were infected with 1×10^4 focus-forming units (FFU) of the ZIKV by retroorbital injection. Pathological symptoms and signs (**Figure 1A**), as well as weight changes (**Figure 1B**), were observed in the *lfnar1*^{-/-} mice after an infection with the ZIKV. The murine brains showed obvious edema and hyperemia (**Figure 1C**). Meanwhile, the testes shrank gradually (**Figure 1D**). Furthermore, pathological changes and the destruction of tissue were found in the brain and testes (**Figure 2A**). We performed an immunofluorescence assay to detect the ZIKV in the brain and testes (**Figure 2B**). High viral loads were detected in the brain and testis by immunostaining (**Figure 2B**). Immunohistochemistry showed a robust infiltration of CD3⁺ T cells into the mice brain after the infection with the ZIKV (**Figure 2C**).

To detect and evaluate ZIKV-specific T-cell responses, we prepared a mouse MHC-I H-2D^b-E₂₉₄₋₃₀₂ tetramer. The peptide E₂₉₄₋₃₀₂ can help the H-2D^b renature properly and yield a high amount of the soluble MHC-I (**Figure 3A**). In the shift assay, a high efficiency in biotinylation could be observed (**Figure 3B**). Subsequently, three streptavidin fluorescence (APC, PE, and BV421)-tagged pMHC-I tetramers were produced to detect ZIKV-specific T cells (**Figure 3C**). The PE-labeled tetramer had a higher efficacy to detect the specific CD8⁺ T cell compared to the APC- and BV421-labeled tetramers, though the difference was not statistically significant.

Using the E₂₉₄₋₃₀₂ tetramer, we detected ZIKV-specific T lymphocytes in the spleen of the infected mice by flow cytometry at 7 d post-inoculation of the ZIKV ($3.49 \pm 0.45\%$). Also, similar to the method described in section 3 of this protocol, with 4 weeks post-immunization of AdC7-M/E vaccine, ZIKV-specific T lymphocytes were detected in the spleen ($6.89 \pm 1.36\%$) (**Figure 4**).

Furthermore, we detected the lymphocytes infiltrated into the immunoprivileged organs, such as the brain and testes, after the ZIKV infection. The gates were set to select for CD3⁺CD8⁺ T cells in total lymphocytes of the brain and testes. A high ratio of the E₂₉₄₋₃₀₂ tetramer-specific T cells could be detected in the brain (42.2% in CD3⁺CD8⁺ T cells) and the testicular (26.4% in CD3⁺CD8⁺ T cells) lymphocytes (**Figure 5**).

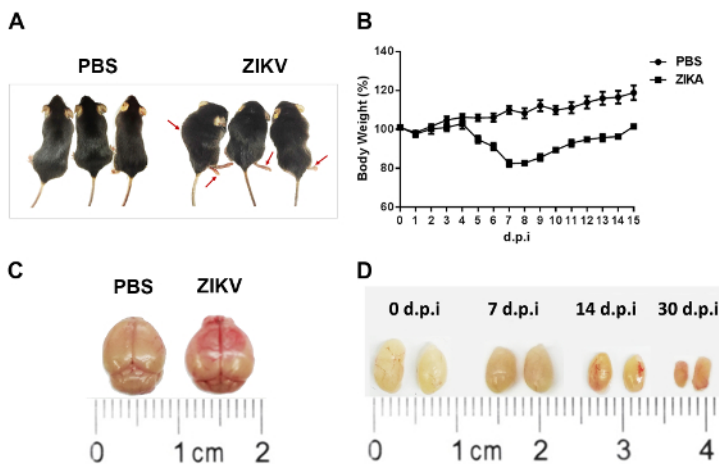


Figure 1: Characterization of the ZIKV infection in *lfnar1*^{-/-} mice. *lfnar1*^{-/-} mice at 6–8 weeks of age were infected with 10^4 focus-forming units (FFU) of the ZIKV by retroorbital injection, and mice injected with PBS were used as uninfected controls. The (A) morphology and (B) weight changes of infected *lfnar1*^{-/-} mice were monitored. The red arrows indicate *lfnar1*^{-/-} mice presented with myeloparalysis and motor paraparesis after the infection. (C) Brains at 7 d post-inoculation and (D) testes at 0, 7, 14, and 30 days post-inoculation were harvested. Representative images of the brain and testes from the mice are shown with a ruler to indicate the sizes. The error bars represent the mean \pm SEM. $n = 10$ mice per group per experiment. [Please click here to view a larger version of this figure.](#)

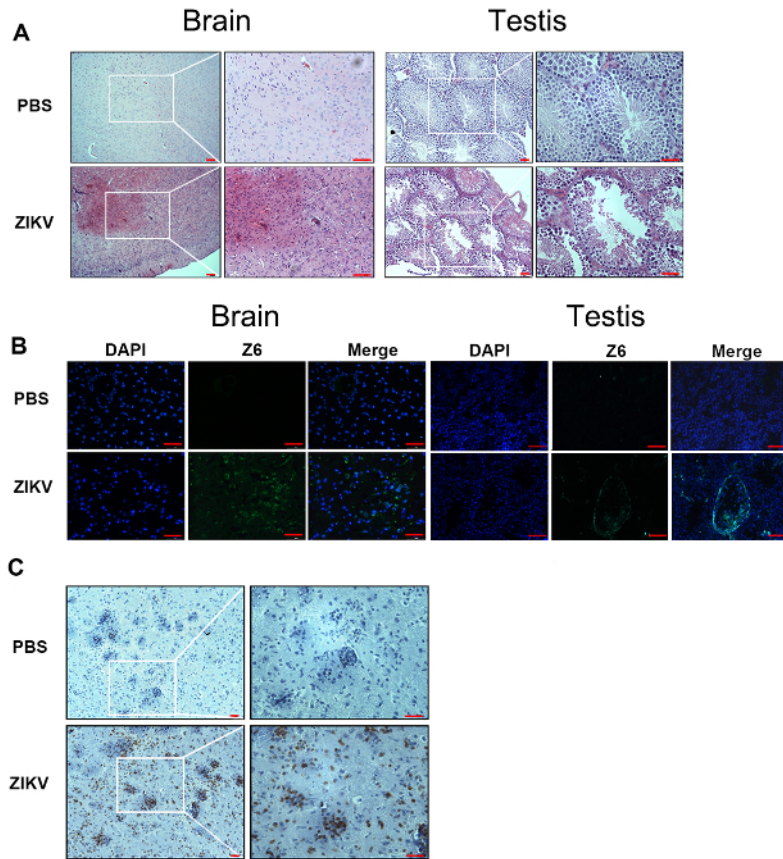


Figure 2: Detection of the ZIKV and lymphocytes in the brain and testis of ZIKV-infected *Ifnar1^{-/-}* mice. (A) This panel shows histopathological changes in the brain and testes from ZIKV-infected mice compared with negative controls at 7 d post-inoculation. Scale bar = 25 μ m (left panel) and 50 μ m (right panel). (B) An immunofluorescence assay was performed with the anti-ZIKV Z6 antibody (green). All tissue samples were collected from ZIKV-infected mice at 7 d post-inoculation. The nuclei were stained with DAPI (blue). Scale bar = 50 μ m. (C) Immunohistochemistry shows a robust infiltration of CD3⁺ T cells into the brain and testis. Scale bar = 25 μ m (left panel) and 50 μ m (right panel). Purple indicates hematoxylin, brown represents the CD3 antibody. [Please click here to view a larger version of this figure.](#)

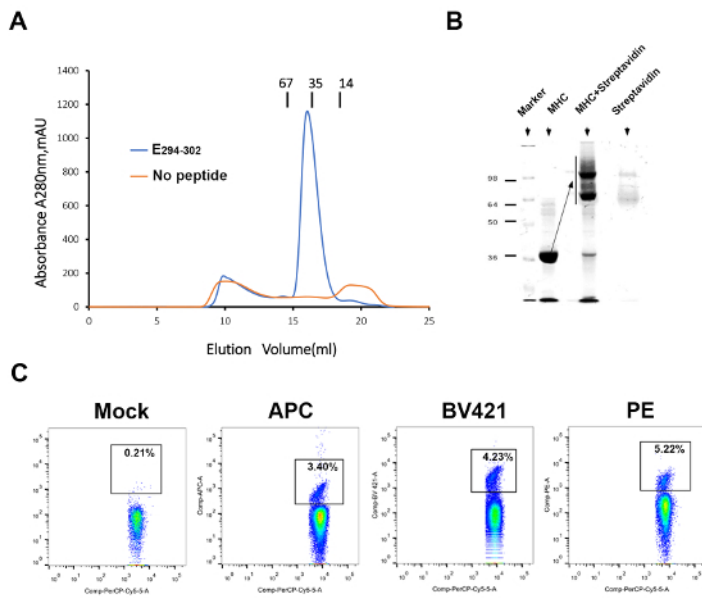


Figure 3: Preparation of ZIKV-specific pMHC-I tetramers. (A) The binding of E₂₉₄₋₃₀₂ to H-2D^b is elucidated by an *in vitro* refolding. Blue indicates the H-2D^b-E₂₉₄₋₃₀₂ protein. Orange represents the negative control without peptide. (B) This panel shows the H-2D^b-E₂₉₄₋₃₀₂ shift assay. (C) The mock represents a PBS control. Three streptavidin fluorescence (APC, PE, and BV421)-tagged pMHC-I tetramers were used to detect ZIKV-specific T cells. [Please click here to view a larger version of this figure.](#)

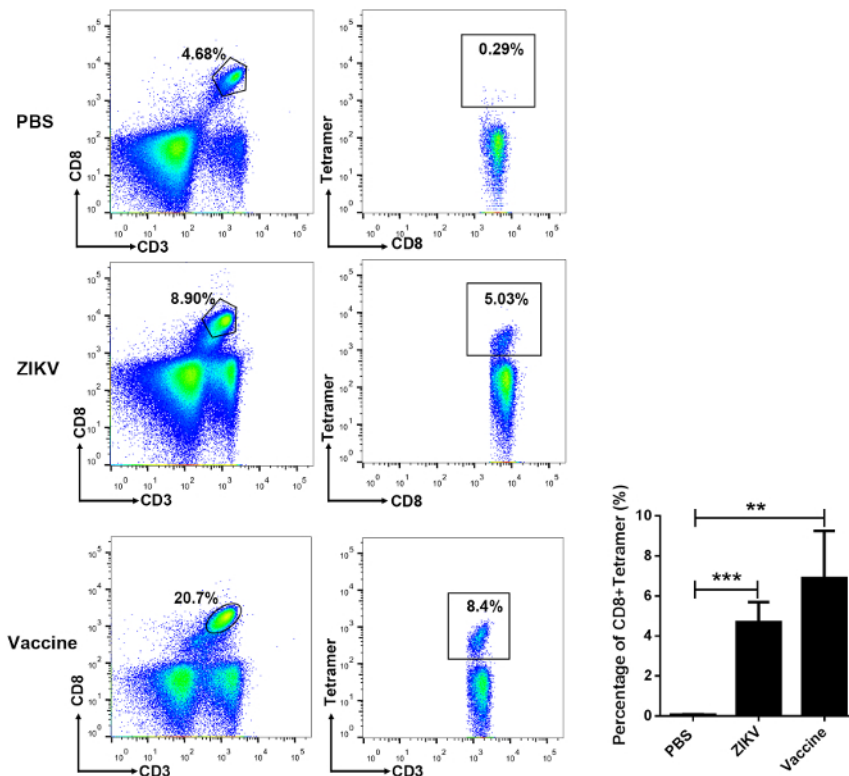


Figure 4: Flow cytometric analysis of virus-specific CD8⁺ T cells in the spleen of ZIKV-infected and vaccine-immunized mice. Ifnar1^{-/-} mice at 6-8 weeks of age were either infected with 10⁴ focus-forming units (FFU) of ZIKV or received a single-dose of 4 x 10¹⁰ viral particles of AdC7-M/E or PBS as a negative control. After 7 days post-infection or 4 weeks post-vaccination, mouse splenocytes were harvested and analyzed by flow cytometry. The data are shown as mean ± SD. Statistical analysis was performed using one-way ANOVA (not significant: *P* > 0.05; **P* < 0.05; ***P* < 0.01; ****P* < 0.001; *****P* < 0.0001). [Please click here to view a larger version of this figure.](#)

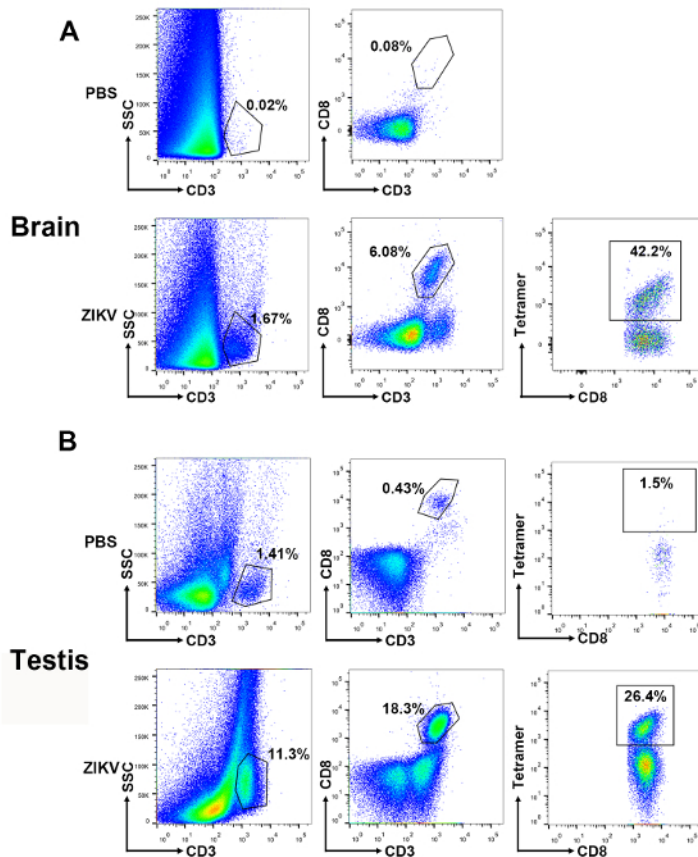


Figure 5: Gating strategy and representative results of virus-specific CD8⁺ T cells in the brain and testes of ZIKV-infected mice. Representative plots are shown for the infiltrated lymphocytes in (A) the brain and (B) the testes. A succession of gates is set to select lymphoid-scatter⁺ and CD3⁺ events. Of these, CD8⁺ events are gated for the analysis of epitope-specific T cells. [Please click here to view a larger version of this figure.](#)

Discussion

Immunogenic T-cell epitope plays a significant role in cellular immunity against pathogens²³. Thus, the detection of ZIKV-specific T cells in immunoprivileged organs is a critical methodology to understand T-cell responses against the natural ZIKV infection. Meanwhile, T-cell response detection is an excellent tool to investigate the efficacy of the viral vaccine. Here, we show a comprehensive protocol to visualize the experiments, which include the isolation of lymphocytes from the spleen, brain, and testes of ZIKV-infected mice, the preparation of the immunodominant epitope E₂₉₄₋₃₀₂ tetramer, and the recognition of ZIKV-specific CD8⁺ T cells in immunoprivileged organs of ZIKV-infected mice.

A previous study showed that a live ZIKV or its RNA can be detected in the semen of male patients, which indicates that the ZIKV can bypass the blood-testis barrier and replicate itself in the reproductive system²⁴. Previously, we also showed that the ZIKV can cause testes damage and lead to male infertility in mice²⁵. ZIKV infection can lead to viremia in rhesus monkeys, and the viral RNA can be detected in the central nervous system (CNS), as well as in the visceral organs. Immunohistochemistry revealed that ZIKV-specific antigens were presented in the CNS and the multiple peripheral organs²⁶. Also, in murine models, ZIKV infection can induce a robust antiviral CD8⁺ T-cell response in the spleen and CNS²⁶.

Compared to previous work, this study establishes systematic methods to detect ZIKV-specific CD8⁺ T-cell responses in the brain and testes, which are immunoprivileged sites. It is important to assess the functionality of virus-specific T cells in the immunoprivileged organs of the ZIKV-infected mice. The usage of tetramers to detect ZIKV-specific CD8⁺ T-cell responses in immunoprivileged organs would greatly enhance our understanding of ZIKV infections and their host immune responses. Using E₂₉₄₋₃₀₂ tetramer, virus-specific T cells in brain and testes can be isolated by flow cytometry, to investigate the cellular mechanisms of the protection and immunopathogenesis during a ZIKV infection. Meanwhile, it is helpful for researchers to investigate further the functions of the CD8⁺ T cells to control the ZIKV, or to enhance the immunopathogenesis in these organs during ZIKV infection.

To analyze the antigen-specific murine CD8⁺ T-cell responses in the immunoprivileged organs, we prepared H-2D^b-E₂₉₄₋₃₀₂ tetramer and detected the CD8⁺ T cells by flow cytometry. Tetramers are a powerful tool to detect antigen-specific T cells. Here, three types of fluorochrome-conjugated streptavidin (APC, PE, and BV421) were generated. Although there are no statistically significant differences in the APC-, BV421-, and PE-labeled tetramers for detecting antigen-specific T cells, PE-labeled pMHC-I tetramers yielded the best results. Hence, the PE-labeled tetramer was used throughout this study. Interestingly, based on the PE-labeled H-2D^b-E₂₉₄₋₃₀₂ tetramer, we detected high ratios of antigen-

specific T cells in both the brain and testes, which indicate the migration ability of the virus-specific T cells from the blood to immunoprivileged organs.

However, there are some limitations to the protocol. The H-2D^b-E₂₉₄₋₃₀₂ tetramer is not useful for human T-cell detection, because tetramer detection is dependent on MHC restriction. The screening of immunodominant HLA-restricted peptides is still needed. Besides, retro-orbital infection is effective for a ZIKV infection but might be not a convenient operation for some investigators. Thus, other routes of infection, including peritoneal, subcutaneous, or intravenous, are also recommended.

In the protocol described here, a critical step is the isolation of monocytes from brain and testis. It is important to acquire high-quality lymphocytes; thus, it is important to pay attention to, for example, the centrifugal speed, the strength of the grinding tissue, and the dissection of the brain and testis tissue. Besides, for tetramer preparation, protease inhibitors (PMSF, pepstatin, leupeptin) are helpful when protecting a protein from being degraded. Therefore, it makes sense to add a protease inhibitor to the refolding buffer and exchange the buffer during the process of the tetramer preparation.

In conclusion, we present the methods of detecting antigen-specific T-cell responses in the immunoprivileged organs of the *lfnr1*^{-/-} mouse model for a ZIKV infection. This platform can be widely applied to investigate the immune mechanisms of emerging and re-emerging viruses which can bypass the barriers between the blood and the immunoprivileged organs. Moreover, this study may pave the way for the future development of candidate vaccines and immunotherapies.

Disclosures

The authors have nothing to declare.

Acknowledgements

The authors thank Gary Wong for the English revision. This work was supported by the National Key Research and Development Program of China (grant 2017YFC1200202), the Major Special Projects for Infectious Disease Research of China (grant 2016ZX10004222-003). George F. Gao is a leading principal investigator of the National Natural Science Foundation of China Innovative Research Group (grant 81621091).

References

- Dick, G. W., Kitchen, S. F., Haddow, A. J. Zika virus. I. Isolations and serological specificity. *Transactions of the Royal Society of Tropical Medicine and Hygiene*. **46** (5), 509-520 (1952).
- Hazin, A. N. *et al.* Computed Tomographic Findings in Microcephaly Associated with Zika Virus. *The New England Journal of Medicine*. **374** (22), 2193-2195 (2016).
- Zhang, Y. *et al.* Highly diversified Zika viruses imported to China, 2016. *Protein & Cell*. **7** (6), 461-464 (2016).
- Cauchemez, S. *et al.* Association between Zika virus and microcephaly in French Polynesia, 2013-15: a retrospective study. *The Lancet*. **387** (10033), 2125-2132 (2016).
- Turtle, L. *et al.* Human T cell responses to Japanese encephalitis virus in health and disease. *The Journal of Experimental Medicine*. **213** (7), 1331-1352 (2016).
- Dudley, D. M. *et al.* A rhesus macaque model of Asian-lineage Zika virus infection. *Nature Communications*. **7**, 12204 (2016).
- Osuna, C. E. *et al.* Zika viral dynamics and shedding in rhesus and cynomolgus macaques. *Nature Medicine*. **22** (12), 1448-1455 (2016).
- Stettler, K. *et al.* Specificity, cross-reactivity, and function of antibodies elicited by Zika virus infection. *Science*. **353** (6301), 823-826 (2016).
- Zhao, M., Zhang, H., Liu, K., Gao, G. F., Liu, W. J. Human T-cell immunity against the emerging and re-emerging viruses. *Science China Life Sciences*. **60** (12), 1307-1316 (2017).
- Huang, H. *et al.* CD8+ T Cell Immune Response in Immunocompetent Mice during Zika Virus Infection. *Journal of Virology*. **91** (22), e00900-17 (2017).
- Elong Ngonu, A. *et al.* Mapping and Role of the CD8+ T Cell Response During Primary Zika Virus Infection in Mice. *Cell Host & Microbe*. **21** (1), 35-46 (2017).
- Marques, E. T. A., Burke, D. S. Tradition and innovation in development of a Zika vaccine. *The Lancet*. **391** (10120), 516-517 (2017).
- Xu, K. *et al.* Recombinant Chimpanzee Adenovirus Vaccine AdC7-M/E Protects against Zika Virus Infection and Testis Damage. *Journal of Virology*. JVI.01722-17 (2018).
- Jama, B. P., Morris, G. P. Generation of human alloantigen-specific T cells from peripheral blood. *Journal of Visualized Experiments*. (93), e52257 (2014).
- Legoux, F. P., Moon, J. J. Peptide:MHC tetramer-based enrichment of epitope-specific T cells. *Journal of Visualized Experiments*. (68), e4420 (2012).
- Govindarajan, S., Elewaut, D., Drennan, M. An Optimized Method for Isolating and Expanding Invariant Natural Killer T Cells from Mouse Spleen. *Journal of Visualized Experiments*. (105), e53256 (2015).
- Posel, C., Moller, K., Boltze, J., Wagner, D. C., Weise, G. Isolation and Flow Cytometric Analysis of Immune Cells from the Ischemic Mouse Brain. *Journal of Visualized Experiments*. (108), e53658 (2016).
- John D. Altman, P. A. H. M., Mark M. Davis. Phenotypic Analysis of Antigen-Specific T Lymphocytes. *science*. **274** 94-96 (1996).
- Li, H., Zhou, M., Han, J., Zhu, X., Dong, T., Gao, G.F., Tien, P. Generation of murine CTL by a hepatitis B virus-specific peptide and evaluation of the adjuvant effect of heat shock protein glycoprotein 96 and its terminal fragments. *J Immunol*. **174** (1), 195-204 (2005).
- Valkenburg, S. A. *et al.* Preemptive priming readily overcomes structure-based mechanisms of virus escape. *Proceedings of the National Academy of Sciences of the United States of America*. **110** (14), 5570-5575 (2013).
- Shang, T. *et al.* Toll-like receptor-initiated testicular innate immune responses in mouse Leydig cells. *Endocrinology*. **152** (7), 2827-2836 (2011).

22. Evilsizor, M. N., Ray-Jones, H. F., Lifshitz, J., Ziebell, J. Primer for immunohistochemistry on cryosectioned rat brain tissue: example staining for microglia and neurons. *Journal of Visualized Experiments*. (99), e52293 (2015).
23. Zhou, M. *et al.* Screening and identification of severe acute respiratory syndrome-associated coronavirus-specific CTL epitopes. *The Journal of Immunology*. **177** (4), 2138-2145 (2006).
24. Barzon, L., Lavezzo, E., Palu, G. Zika virus infection in semen: effect on human reproduction. *The Lancet Infectious Diseases*. **17** (11), 1107-1109 (2017).
25. Ma, W. *et al.* Zika Virus Causes Testis Damage and Leads to Male Infertility in Mice. *Cell*. **167** (6), 1511-1524, e1510 (2016).
26. Li, X. F. *et al.* Characterization of a 2016 Clinical Isolate of Zika Virus in Non-human Primates. *EBioMedicine*. **12**, 170-177 (2016).